Research Article

For reprint orders, please contact: reprints@future-science.com

Future Medicinal Chemistry

Isoform selectivity of harmine-conjugated 1,2,3-triazoles against human monoamine oxidase

Saqlain Haider[1], Manal Alhusban[2], Narayan D Chaurasiya[1], Babu L Tekwani[1], Amar G Chittiboyina*,[1] & Ikhlas A Khan[1]

[1]National Center for Natural Products Research, School of Pharmacy, The University of Mississippi, MS 38677, USA

[2]Division of Pharmacognosy, Division of Pharmacology, Department of BioMolecular Sciences, School of Pharmacy, The University of Mississippi, MS 38677, USA

*Author for correspondence: Tel.: +1 662 915 1572; Fax: +1 662 915 7989; amar@olemiss.edu

Aim: There is little information available on the monoamine oxidase isoform selectivity of *N*-alkyl harmine analogs, which exhibit a myriad of activities including MAO-A, DYRK1A and cytotoxicity to several select cancer cell lines. **Results:** Compounds **3e** and **4c** exhibited an IC_{50} of 0.83 ± 0.03 and 0.43 ± 0.002 μM against MAO-A and an IC_{50} of 0.26 ± 0.04 and 0.36 ± 0.001 μM against MAO-B, respectively. Molecular docking studies revealed π–π interactions between the synthesized molecules and aromatic amino acid residues. **Conclusion & future perspective:** The current study delineates the structural requirements for MAO-A selectivity and such information may be helpful in designing selective analogs for kinase, DYRK1A and harmine-based cytotoxics without apparent MAO enzyme inhibition.

First draft submitted: 8 January 2018; Accepted for publication: 16 March 2018; Published online: 23 May 2018

Keywords: 1,2,3-triazoles • click chemistry • harmine • monoamine oxidase

Indole alkaloids, also known as carboline alkaloids, are a large group of secondary metabolites ubiquitously found in nature, including various plants, insects and mammalians as well as human tissues and body fluids. Harmine is a naturally occurring β-carboline alkaloid, which was first reported in 1847 from *Peganum harmala* and *Banisteriopsis caapi*, both of which have been traditionally used for remedial preparations in central Asia, Middle East and South America [1,2]. Harmine has also been reported to be present in human tissues and plant-derived foods as a natural metabolite [3]. Several carboline alkaloids including harmine have been established as pharmaceutically important molecules associated with a broad spectrum of biological activities namely, antiviral, hallucinogenic, antitumor and antiparasitic activities [4]. Pharmacological and therapeutic effects of harmala alkaloids were delineated by Moloudizargari *et al.* [4]. Moreover, harmine (Figure 1) was reported to possess selective, potent inhibition against biological targets, dual-specificity DYRK1A and MAO-A and their respective x-ray structures have been reported [5–8]. Ogawa and his team demonstrated the development of a novel selective inhibitor of Down syndrome-related kinase DYRK1A in 2010 [5].

Monoamine oxidases belong to the family of FAD-containing enzymes which are distributed on the outer membrane of mitochondria present in gut mucosa, nerve cells, liver and other tissues [9]. Both the isoforms of MAO are encoded by the different genes present on the X chromosome and constitute approximately 70% amino acid homologous identity [10–12]. Hydrogen peroxide is produced as a byproduct in the neuronal tissues as a result of increased levels of MAO, resulting in an increase in the amount of reactive oxygen species which plays a key role in the pathogenesis of neurodegenerative diseases. Therefore, the MAO inhibitors are considered as potent drug candidates for the treatment of neurodegenerative diseases [13]. Both isoforms of MAO are associated in the oxidative deamination of biogenic and xenobiotic amines into corresponding aldehydes and ammonia [14]. The two isoforms of MAO differ from each other on the basis of their substrate and inhibitor specificity.

MAO-A is known to catalyze the deamination of noradrenaline, serotonin and adrenaline, and it is selectively inhibited by moclobemide and clorgyline. Whereas MAO-B is involved in the preferential deamination of benzy-

newlands press

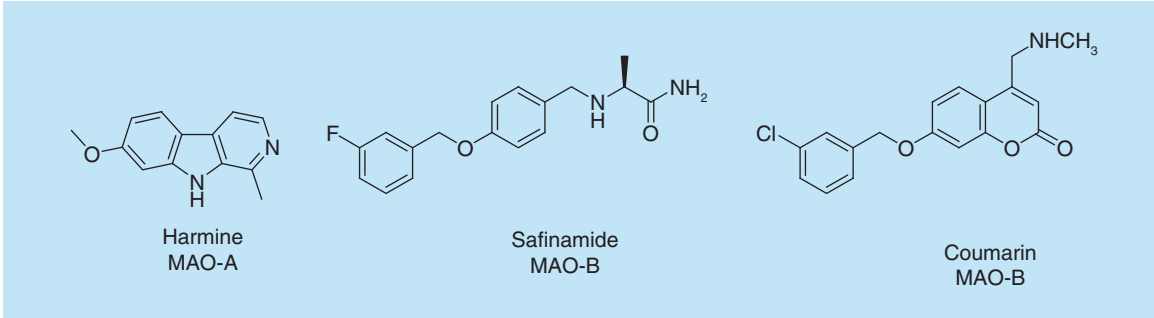

Figure 1. Selective inhibitors of MAO-A and MAO-B isozymes.

lamine and β-phenylethylamine and is selectively inhibited by selegiline [14]. Dopamine is subjected to deamination preferentially with MAO-B. The treatment for anxiety and mental depression involves MAO-A inhibitors and that for Parkinson's disease involves selective MAO-B inhibitors (Figure 1) [15]. Therefore, the two isoforms of MAO are attractive therapeutic targets for the treatment of several neurological disorders.

The crystal structure of MAO-B I complex with safinamide and two coumarin analogs, all sharing a common, benzyloxy, functional group is reported by Mattevi *et al.* [15]. Keeping in mind the selective inhibitory activity of harmine on MAO-A over MAO-B (>10,000-fold selectivity) we have designed the synthesis of single and double methylene-bridged 1,2,3-triazole derivatives through simple 'click' chemistry and screened them for their MAO inhibitory potentials [6]. Due to their extensive biological activities, ease of multigram scale synthesis, atom economy, ready availability of reactants, the heterocyclic pharmacophore, 1,2,3-triazole, was selected to tether to the harmine scaffold via click chemistry [16,17]. The key compounds exhibiting MAO inhibition have been subjected to *in silico* molecular docking studies against MAO-A and -B to get additional insights on the observed biological activities and selectivity against individual MAO isoforms.

Experimental

Chemistry

All the chemicals and reagents were purchased from Sigma Aldrich (MO, USA). All the IR spectra were recorded on an Agilent 630 FTIR (Agilent Technologies, CA, USA). ^{1}H and ^{13}C NMR spectra were determined on Bruker (400 and 500 MHz; Bruker Biospin, MA, USA) spectrometers and chemical shifts were expressed as p.p.m. against tetramethyl silane as internal reference. Mass spectra were recorded on Agilent 1290 UHPLC and 6120 MS (Agilent Technologies), and column chromatography was performed on (Merck, MA, USA) silica gel 60. All compounds prepared in this paper are novel and their formation has been confirmed from the spectral data. The propargyl derivatives (1.0 mmol; **1a**–**1d**) were dissolved in 10 ml of tetrahydrofuran:water (THF:H_2O) (1:1) at room temperature. $CuSO_4.5H_2O$ (1.2 mmol) was charged into it and the reaction mixture was stirred for 10 min at the room temperature. The reaction mixture became light blue in color. Sodium ascorbate (5.0 mmol) was then added to the reaction mixture and stirred for 15 min. The color of the reaction mixture then changed to dark yellow. After 10 min, aromatic azides (1.2 mmol) were added into the reaction mixture. The reaction mixture was then allowed to stir further for 5–8 h at room temperature. After completion of the reaction, monitored by the TLC, reaction mixture was quenched with water and extracted with ethyl acetate. Combined organic layers were dried over anhydrous sodium sulfate, filtered and concentrated under reduced pressure to obtain the final crude products which were purified with flash column chromatography.

1-Methyl-9-(3-phenylpropyl)-7-(prop-2-yn-1-yloxy)-9H-pyrido[3,4-b]indole (1a)

White powder; yield 88%; ^{1}H NMR (500 MHz, $CDCl_3$): δ 2.14–2.19 (m, 2H), 2.57 (t, 1H, J = 2.4 Hz), 2.78 (t, 2H, J = 7.4 Hz), 2.91 (s, 3H), 4.44–4.46 (m, 2H), 4.76 (d, 2H, J = 2.4 Hz), 6.80 (d, 1H, J = 2.1 Hz), 6.94 (dd, 1H, J = 8.6, 2.2 Hz), 7.22–7.26 (m, 3H), 7.33–7.36 (m, 2H), 7.74 (d, 1H, J = 5.2 Hz), 7.99 (d, 1H, J = 8.6 Hz), 8.29 (d, 1H, J = 5.2 Hz); ^{13}C NMR (125 MHz, $CDCl_3$): δ 23.17, 31.80, 33.01, 44.21, 56.23, 75.81, 78.44, 94.66, 109.36, 112.37, 115.88, 122.45, 126.37, 128.42, 128.64, 129.23, 135.34, 138.30, 140.70, 158.55; ESI^{+}-MS: 355.18 $[M+H]^{+}$ for $C_{24}H_{23}N_2O$.

1-Methyl-7-(prop-2-yn-1-yloxy)-9-propyl-9H-pyrido[3,4-b]indole (1b)

Whitish yellow powder; yield 90%; ^{1}H NMR (500 MHz, $CDCl_3$): δ 1.00 (t, 3H, *J* = 7.4 Hz), 1.81–1.86 (m, 2H), 2.60 (t, 1H, *J* = 2.4 Hz), 3.00 (s, 3H), 4.37–4.40 (m, 2H), 4.83 (d, 2H, *J* = 2.3 Hz), 6.93 (dd, 1H, *J* = 8.5, 2.2 Hz), 6.96 (d, 1H, *J* = 2.1 Hz), 7.73 (d, 1H, *J* = 5.2 Hz), 7.97 (d, 1H, *J* = 8.5 Hz), 8.28 (d, 1H, *J* = 5.2 Hz); ^{13}C NMR (125 MHz, $CDCl_3$): δ 11.32, 23.39, 23.96, 46.35, 56.26, 75.92, 78.46, 94.99, 108.92, 112.40, 115.78, 122.41, 129.10, 135.37, 138.15, 140.66, 142.78, 158.48. ESI$^+$-MS: 279.15 $[M+H]^+$ for $C_{18}H_{19}N_2O$.

9-Butyl-1-methyl-7-(prop-2-yn-1-yloxy)-9H-pyrido[3,4-b]indole (1c)

Yellow powder; yield 92%; ^{1}H NMR (400 MHz, $CDCl_3$): δ 1.01 (t, 3H, *J* = 7.4 Hz), 1.43–1.49 (m, 2H), 1.82–1.87 (m, 2H), 2.59 (t, 1H, *J* = 2.4 Hz), 3.05 (s, 3H), 4.47–4.50 (m, 2H), 4.86 (d, 2H, *J* = 2.4 Hz), 6.96 (dd, 1H, *J* = 8.6, 2.2 Hz), 7.02 (d, 1H, *J* = 2.2 Hz), 7.77 (d, 1H, *J* = 5.2 Hz), 8.02 (d, 1H, *J* = 8.6 Hz), 8.29 (d, 1H, *J* = 5.2 Hz); ^{13}C NMR (100 MHz, $CDCl_3$): δ 13.91, 20.21, 23.27, 32.76, 44.75, 56.33, 75.81, 78.49, 95.12, 108.96, 112.35, 115.91, 122.39, 135.40, 138.16, 140.68, 142.82, 158.56. ESI$^+$-MS: 293.16 $[M+H]^+$ for $C_{19}H_{21}N_2O$.

9-Isobutyl-1-methyl-7-(prop-2-yn-1-yloxy)-9H-pyrido[3,4-b]indole (1d)

White powder; yield 85%; ^{1}H NMR (400 MHz, $CDCl_3$): δ 0.95 (d, 6H, *J* = 6.6 Hz), 2.24–2.29 (m, 1H), 2.59 (t, 1H, *J* = 2.4 Hz), 3.02 (s, 3H), 4.29 (d, 2H, *J* = 7.4 Hz), 4.84 (d, 2H, *J* = 2.4 Hz), 6.95 (dd, 1H, *J* = 8.6, 2.2 Hz), 7.02 (d, 1H, *J* = 2.1 Hz), 7.76 (d, 1H, *J* = 5.2 Hz), 8.00 (d, 1H, *J* = 8.6 Hz), 8.31 (d, 1H, *J* = 5.2 Hz); ^{13}C NMR (100 MHz, $CDCl_3$): δ 20.23, 23.67, 30.58, 51.90, 56.32, 75.84, 78.54, 95.79, 109.09, 112.31, 115.77, 122.28, 129.26, 135.70, 138.29, 140.80, 143.29, 158.41. ESI$^+$-MS: 293.16 $[M+H]^+$ for $C_{19}H_{21}N_2O$.

7-((1-Benzyl-1H-1,2,3-triazol-4-yl)methoxy)-1-methyl-9-(3-phenylpropyl)-9H-pyrido[3,4-b]indole (2a)

Brown powder; yield 78%; IR: ν (cm^{-1}) 1619, 1559, 1449, 1203, 1161; ^{1}H NMR (400 MHz, $CDCl_3$): δ 1.99–2.15 (m, 2H), 2.74 (t, *J* = 7.3 Hz, 2H), 2.88 (s, 3H), 4.39–4.43 (m, 2H), 5.24 (s, 2H), 5.53 (s, 2H), 6.81 (d, 1H, *J* = 2.1 Hz), 6.91 (dd, 1H, *J* = 8.6, 1.9 Hz), 7.15–7.25 (m, 4H), 7.29–7.34 (m, 3H), 7.35–7.40 (m, 3H), 7.60 (s, 1H), 7.71 (s, 1H), 7.94 (d, 1H, *J* = 8.5 Hz,), 8.28 (s, 1H); ^{13}C NMR (100 MHz, $CDCl_3$): δ 23.03, 31.85, 32.96, 44.16, 54.28, 62.46, 94.37, 109.58, 115.45, 122.46, 122.77, 126.39, 128.15, 128.37, 128.45, 128.63, 128.85, 129.16, 129.32, 129.39, 134.44, 140.66, 142.90, 159.38; ESI$^+$-MS: 488.25 $[M+H]^+$ for $C_{31}H_{30}N_5O$.

1-Methyl-7-((1-(4-methylbenzyl)-1H-1,2,3-triazol-4-yl)methoxy)-9-(3-phenylpropyl)-9H-pyrido[3,4-b]indole (2b)

White yellow powder; yield 80%; IR: ν (cm^{-1}) 1720, 1619, 1559, 1410, 1241; ^{1}H NMR (500 MHz, $CDCl_3$): δ 2.10–2.16 (m, 2H), 2.36 (s, 3H), 2.75 (t, 2H, *J* = 7.4 Hz), 2.90 (s, 3H), 4.43–4.47 (m, 2H), 5.25 (s, 2H), 5.50 (s, 2H), 6.83 (d, 1H, *J* = 2.1 Hz), 6.91–6.94 (m, 1H), 7.18–7.25 (m, 7H), 7.31–7.34 (m, 2H), 7.57 (s, 1H), 7.73–7.76 (m, 1H), 7.96 (d, 1H, *J* = 8.6 Hz), 8.29 (d, 1H, *J* = 5.3 Hz); ^{13}C NMR (125 MHz, $CDCl_3$): δ 19.18, 21.18, 32.98, 33.13, 54.12, 62.49, 71.82, 94.39, 109.61, 112.40, 115.45, 122.47, 122.61, 126.40, 128.22, 128.45, 128.63, 128.85, 129.82, 130.94, 131.36, 137.97, 138.84, 140.65, 142.93, 144.28, 159.40; ESI$^+$-MS: 502.26 $[M+H]^+$ for $C_{32}H_{32}N_5O$.

7-((1-(4-Bromobenzyl)-1H-1,2,3-triazol-4-yl)methoxy)-1-methyl-9-(3-phenylpropyl)-9H-pyrido[3,4-b]indole (2c)

Brown powder; yield 80%; IR: ν (cm^{-1}) 1621, 1561, 1448, 1243, 1203; ^{1}H NMR (400 MHz, $CDCl_3$): δ 2.12–2.19 (m, 2H), 2.77 (t, 2H, *J* = 7.3 Hz), 2.91 (s, 3H), 4.48 (t, 2H, *J* = 8.0 Hz), 5.28 (s, 2H), 5.69 (s, 2H), 6.86 (d, *J* = 1H, 2.2 Hz), 6.94 (dd, 1H, *J* = 8.6, 2.1 Hz), 7.22–7.27 (m, 6H), 7.30–7.36 (m, 3H), 7.46 (dd, 1H, *J* = 7.9, 1.3 Hz), 7.70 (s, 1H), 7.98 (d, 1H, *J* = 8.5 Hz), 8.30 (s, 1H); ^{13}C NMR (100 MHz, $CDCl_3$): δ 31.89, 33.00, 44.23, 51.54, 62.50, 109.57, 122.46, 126.40, 127.64, 128.45, 128.63, 129.98, 130.37, 130.49, 132.27, 133.57, 140.66, 259.34; ESI$^+$-MS: 566.16 $[M+H]^+$ for $C_{31}H_{29}BrN_5O$.

4-((4-(((1-Methyl-9-(3-phenylpropyl)-9H-pyrido[3,4-b]indol-7-yl)oxy)methyl)-1H-1,2,3-triazol-1-yl)methyl)benzonitrile (2d)

White powder; yield 82%; IR: ν (cm^{-1}) 1623, 1563, 1446, 1224, 1166; ^{1}H NMR (400 MHz, $CDCl_3$): δ 2.06–2.16 (m, 2H), 2.74 (t, 2H, *J* = 7.4 Hz), 2.89 (s, 3H), 4.41–4.45 (m, 2H), 5.26 (s, 2H), 5.59 (s, 2H), 6.81 (d, 1H, *J* = 2.1 Hz), 6.91 (dd, 1H, *J* = 8.6, 2.1 Hz), 7.20–7.25 (m, 3H), 7.30–7.36 (m, 4H), 7.63–7.67 (m, 3H), 7.72 (d,

1H, *J* = 5.2 Hz), 7.95 (d, 1H, *J* = 8.6 Hz), 8.28 (d, 1H, 5.3 Hz); ^{13}C NMR (100 MHz, $CDCl_3$): δ 22.99, 31.89, 32.89, 44.19, 53.47, 62.38, 94.31, 109.49, 112.34, 112.85, 115.56, 118.08, 122.51, 122.97, 126.41, 128.44, 128.64, 129.29, 132.89, 135.23, 138.09, 139.61, 140.61, 140.64, 142.86, 144.89, 159; ESI$^+$-MS: 513.24 $[M+H]^+$ for $C_{32}H_{29}N_6O$.

7-((1-(2-Chlorobenzyl)-1H-1,2,3-triazol-4-yl)methoxy)-1-methyl-9-(3-phenylpropyl)-9H-pyrido[3,4-b]indole (2e)

White yellow powder; yield 83%; IR: ν (cm^{-1}) 1621, 1559, 1449, 1243, 1203; ^{1}H NMR (400 MHz, $CDCl_3$): δ 2.03–2.15 (m, 2H), 2.74 (t, 2H, *J* = 7.4 Hz), 2.88 (s, 3H), 4.40–4.44 (m, 2H), 5.24 (s, 2H), 5.47 (s, 2H), 6.80 (d, 1H, *J* = 2.1 Hz), 6.91 (dd, 1H, *J* = 8.6, 2.1 Hz), 7.08–7.26 (m, 7H), 7.30–7.34 (m, 2H), 7.43–7.52 (m, 2H), 7.59 (s, 1H), 7.94 (d, 1H, *J* = 8.6 Hz); ^{13}C NMR (100 MHz, $CDCl_3$): δ 23.50, 32.86, 32.97, 44.17, 53.55, 62.42, 94.39, 109.55, 115.52, 122.47, 122.71, 123.02, 126.40, 128.44, 128.63, 129.72, 129.91, 132.32, 133.45, 140.65, 142.88, 144.59, 159.29; ESI$^+$-MS: 522.21 $[M+H]^+$ for $C_{31}H_{29}ClN_5O$.

1-Methyl-7-((1-phenyl-1H-1,2,3-triazol-4-yl)methoxy)-9-(3-phenylpropyl)-9H-pyrido[3,4-b]indole (2f)

Brown powder; yield 80%; IR: ν (cm^{-1}) 1623, 1559, 1444, 1237, 1159; ^{1}H NMR (400 MHz, $CDCl_3$): δ 2.06–2.15 (m, 2H), 2.75 (t, 2H, *J* = 7.3 Hz), 2.88 (s, 3H), 4.40–4.44 (m, 2H), 5.33 (s, 2H), 6.86 (d, 1H, *J* = 2.2 Hz), 6.97 (dd, 1H, *J* = 8.5, 2.1 Hz), 7.18–7.23 (m, 3H), 7.26–7.34 (m, 2H), 7.43–7.47 (m, 1H), 7.52 (t, 2H, *J* = 7.7 Hz), 7.68–7.75 (m, 3H), 7.97 (d, 1H, *J* = 8.6 Hz), 8.12 (s, 1H), 8.28 (d, 1H, *J* = 5.3 Hz); ^{13}C NMR (100 MHz, $CDCl_3$): δ 23.04, 31.91, 33.00, 44.21, 62.38, 94.31, 109.56, 112.36, 115.57, 120.57, 121.05, 122.53, 126.39, 128.46, 128.52, 128.64, 128.95, 129.31, 129.81, 136.93, 138.15, 140.66, 140.68, 142.88, 144.74, 159.30; ESI$^+$-MS: 474.22 $[M+H]^+$ for $C_{30}H_{28}N_5O$.

7-((1-(4-Methoxyphenyl)-1H-1,2,3-triazol-4-yl)methoxy)-1-methyl-9-(3-phenylpropyl)-9H-pyrido[3,4-b]indole (2g)

White powder; yield 85%; IR: ν (cm^{-1}) 1617, 1559, 1442, 1410, 1241; ^{1}H NMR (500 MHz, $CDCl_3$): δ 2.05–2.15 (m, 2H), 2.74 (t, 2H, *J* = 7.4 Hz), 2.87 (s, 3H), 3.85 (s, 3H), 4.39–4.43 (m, 2H), 5.31 (s, 2H), 6.85 (d, 1H, *J* = 2.2 Hz), 6.95 (dd, 1H, *J* = 8.6, 2.1 Hz), 6.97–7.01 (m, 2H), 7.20–7.25 (m, 3H), 7.30–7.33 (m, 2H), 7.60–7.63 (m, 2H), 7.71–7.72 (m, 1H), 7.95 (d, 1H, *J* = 8.5 Hz), 8.03 (s, 1H), 8.28 (s, 1H); ^{13}C NMR (125 MHz, $CDCl_3$): δ 22.93, 31.88, 32.97, 44.16, 55.63, 62.36, 94.26, 109.62, 114.78, 115.47, 121.25, 122.16, 122.50, 126.37, 128.46, 128.63, 128.67, 129.32, 130.33, 140.67, 142.89, 144.43, 159.36, 159.90; ESI$^+$-MS: 504.24 $[M+H]^+$ for $C_{31}H_{30}N_5O_2$.

7-((1-(4-Bromophenyl)-1H-1,2,3-triazol-4-yl)methoxy)-1-methyl-9-(3-phenylpropyl)-9H-pyrido[3,4-b]indole (2h)

White powder; yield 84%; IR: ν (cm^{-1}) 1619, 1559, 1496, 1442, 1425, 1162; ^{1}H NMR (500 MHz, $CDCl_3$): δ 2.14–2.20 (m, 2H), 2.78 (t, 2H, *J* = 7.3 Hz), 2.92 (s, 3H), 4.51 (t, 2H, *J* = 7.7 Hz), 5.37 (s, 2H), 6.90 (s, 1H), 6.98 (dd, 1H, *J* = 8.5, 2.1 Hz), 7.23–7.35 (m, 7H), 7.63–7.69 (m, 4H), 8.01 (d, 1H, *J* = 8.5 Hz), 8.10 (s, 1H); ^{13}C NMR (125 MHz, $CDCl_3$): δ 31.94, 33.01, 44.24, 62.33, 94.38, 109.65, 121.93, 122.58, 122.63, 126.42, 128.45, 128.65, 132.97, 135.87, 140.63 159.27; ESI$^+$-MS: 552.14 $[M+H]^+$ for $C_{30}H_{27}BrN_5O$.

7-((1-(4-Chlorophenyl)-1H-1,2,3-triazol-4-yl)methoxy)-1-methyl-9-(3-phenylpropyl)-9H-pyrido[3,4-b]indole (2i)

Brown powder; yield 74%; IR: ν (cm^{-1}) 1619, 1559, 1496, 1443, 1218, 1162; ^{1}H NMR (400 MHz, $CDCl_3$): δ 2.14–2.21 (m, 2H), 2.78 (t, 2H, *J* = 7.5 Hz), 2.92 (s, 3H), 4.49–4.53 (m, 2H), 5.38 (s, 2H), 6.90 (d, 1H, *J* = 2.1 Hz), 6.98 (dd, 1H, *J* = 8.6, 2.1 Hz), 7.23–7.27(m, 3H), 7.30–7.36 (m, 2H), 7.50–7.54 (m, 2H), 7.64–7.73 (m, 2H), 7.75 (d, 1H, *J* = 5.2 Hz), 8.01 (d, 1H, *J* = 8.6 Hz), 8.09 (s, 1H), 8.30 (d, 1H, *J* = 5.2 Hz); ^{13}C NMR (100 MHz, $CDCl_3$): δ 23.12, 31.94, 33.02, 44.26, 62.34, 94.33, 109.51, 112.36, 115.67, 120.87, 121.73, 122.58, 126.40, 128.45, 128.64, 130.01, 134.77, 140.66, 145.08, 159.20; ESI$^+$-MS: 508.19 $[M+H]^+$ for $C_{30}H_{27}ClN_5O$.

7-((1-Benzyl-1H-1,2,3-triazol-4-yl)methoxy)-1-methyl-9-propyl-9H-pyrido[3,4-b]indole (3a)

White powder; yield 86%; IR: ν (cm^{-1}) 2098, 1621, 1559, 1446, 1241, 1189; ^{1}H NMR (500 MHz, CD_3OD): δ 0.98 (t, 3H, *J* = 7.4 Hz), 1.80–1.86 (m, 2H), 3.01 (s, 3H), 4.53 (t, 2H, *J* = 7.7 Hz), 5.35 (s, 2H), 5.64 (s, 2H), 6.97 (dd, 1H, *J* = 8.6, 2.1 Hz), 7.21 (d, 1H, *J* = 2.1 Hz), 7.32–7.38 (m, 5H), 7.92 (s, 1H), 8.06 (d, 1H, *J* = 8.6 Hz), 8.12 (s, 2H); ^{13}C NMR (125 MHz, $CDCl_3$): δ 11.26, 23.95, 46.42, 54.38, 62.55, 109.60, 128.15, 128.88, 129.17, 134.37, 159.45; ESI$^+$-MS: 412.21 $[M+H]^+$ for $C_{25}H_{26}N_5O$.

1-Methyl-7-((1-(4-methylbenzyl)-1H-1,2,3-triazol-4-yl)methoxy)-9-propyl-9H-pyrido[3,4-b]indole (3b)

White powder; yield 84%; IR: ν (cm^{-1}) 1619, 1559, 1440, 1250, 1138; ^{1}H NMR (500 MHz, $CDCl_3$): δ 1.01 (t, 3H, *J* = 7.4 Hz), 1.82–1.90 (m, 2H), 2.36 (s, 3H), 3.04 (s, 3H), 4.38–4.45 (m, 2H), 5.35 (s, 2H), 5.51 (s, 2H), 6.94 (dd, 1H, *J* = 8.6, 2.1 Hz), 7.02 (d, 1H, *J* = 2.2 Hz), 7.19 (s, 4H), 7.58 (s, 1H), 7.76 (s, 1H), 7.98 (d, 1H, *J* = 8.5 Hz), 8.30 (s, 1H); ^{13}C NMR (125 MHz, $CDCl_3$): δ 11.25, 21.17, 23.42, 23.92, 46.42, 54.12, 62.59, 94.85, 109.28, 115.51, 122.43, 122.59, 128.19, 129.81, 131.35, 138.83, 143.07, 144.36, 159.36; ESI$^+$-MS: 426.23 $[M+H]^+$ for $C_{26}H_{28}N_5O$.

7-((1-(4-Bromobenzyl)-1H-1,2,3-triazol-4-yl)methoxy)-1-methyl-9-propyl-9H-pyrido[3,4-b]indole (3c)

Brown powder; yield 84%; IR: ν (cm^{-1}) 1626, 1528, 1507, 1476, 1261; ^{1}H NMR (500 MHz, $CDCl_3$): δ 1.02 (t, 3H, *J* = 7.3 Hz), 1.83–1.87 (m, 2H), 3.04 (s, 3H), 4.44 (t, 2H, *J* = 7.8 Hz), 5.36 (s, 2H), 5.51 (s, 2H), 6.94 (dd, 1H, *J* = 8.5, 2.1 Hz), 7.02 (d, 1H, *J* = 2.1 Hz), 71.6–7.18 (m, 2H), 7.50–7.53 (m, 2H), 7.61 (s, 1H), 7.80 (s, 1H), 8.00 (d, 1H, *J* = 8.6 Hz), 8.34 (s, 1H); ^{13}C NMR (125 MHz, $CDCl_3$): δ 11.26, 19.17, 23.92, 46.43, 53.61, 62.54, 94.89, 109.21, 122.45, 123.06, 129.71, 132.35, 133.41, 159.26; ESI$^+$-MS: 490.12 $[M+H]^+$ for $C_{25}H_{25}BrN_5O$.

4-((4-(((1-Methyl-9-propyl-9H-pyrido[3,4-b]indol-7-yl)oxy)methyl)-1H-1,2,3-triazol-1-yl)methyl)benzonitrile (3d)

Green powder; yield 76%; IR: ν (cm^{-1}) 1621, 1559, 1446, 1250, 1138; ^{1}H NMR (400 MHz, $CDCl_3$): δ 1.00 (t, 3H, *J* = 7.4 Hz), 1.81–1.97 (m, 2H), 3.01 (s, 3H), 4.38–4.42 (m, 2H), 5.35 (s, 2H), 5.61 (s, 2H), 6.92 (dd, 1H, *J* = 8.6, 2.2 Hz), 7.00 (d, 1H, *J* = 2.1 Hz), 7.34–7.36 (m, 2H), 7.62–7.68 (m, 3H), 7.73 (d, 1H, *J* = 5.3 Hz), 7.96 (d, 1H, *J* = 8.6 Hz), 8.28 (d, 1H, *J* = 5.3 Hz); ^{13}C NMR (100 MHz, $CDCl_3$): δ 11.24, 23.10, 23.91, 46.40, 53.48, 62.42, 94.79, 109.16, 112.36, 112.84, 115.58, 118.07, 122.49, 123.02, 128.43, 129.27, 132.89, 137.92, 139.61, 140.57, 143.03, 144.91, 159.24; ESI$^+$-MS: 437.21 $[M+H]^+$ for $C_{26}H_{25}N_6O$.

7-((1-(2-Chlorobenzyl)-1H-1,2,3-triazol-4-yl)methoxy)-1-methyl-9-propyl-9H-pyrido[3,4-b]indole (3e)

Yellow powder; yield 72%; IR: ν (cm^{-1}) 1619, 1558, 1500, 1448, 1235, 1019; ^{1}H NMR (400 MHz, $CDCl_3$): δ 0.97–1.00 (m, 3H), 1.83 (s, 2H), 2.98 (s, 3H), 4.39 (s, 2H), 5.34 (s, 2H), 5.66 (s, 2H), 6.93 (d, 1H, *J* = 8.2 Hz), 7.00 (s, 1H), 7.19–7.43 (m, 6H), 7.74 (s, 1H), 7.96 (d, 1H, *J* = 8.4 Hz); ^{13}C NMR (100 MHz, $CDCl_3$): δ 11.33, 24.01, 46.32, 51.70, 51.72, 62.46, 127.19, 127.65, 126.69, 129.69, 129.79, 129.99, 130.05, 130.42, 130.51, 132.21, 133.58, 159.25; ESI$^+$-MS: 446.17 $[M+H]^+$ for $C_{25}H_{25}ClN_5O$.

7-((1-(4-Bromophenyl)-1H-1,2,3-triazol-4-yl)methoxy)-1-methyl-9-propyl-9H-pyrido[3,4-b]indole (3f)

Yellow powder; yield 74%; IR: ν (cm^{-1}) 1625, 1559, 1504, 1444, 1408, 1183; ^{1}H NMR (400 MHz, $CDCl_3$): δ 1.03 (t, 3H, *J* = 7.4 Hz), 1.83–1.95 (m, 2H), 3.04 (s, 3H), 4.43–4.47 (m, 2H), 5.47 (s, 2H), 7.00 (dd, 1H, *J* = 8.6, 2.1 Hz), 7.07 (d, 1H, *J* = 2.2 Hz), 7.64–7.69 (m, 4H), 7.78 (s, 1H), 8.02 (d, 1H, *J* = 8.6 Hz), 8.11 (s, 1H), 8.32 (s, 1H); ^{13}C NMR (100 MHz, $CDCl_3$): δ 11.27, 23.41, 23.94, 46.45, 62.42, 94.85, 109.16, 115.70, 120.84, 121.95, 122.48, 122.56, 122.65, 132.97, 143.07, 145.13, 159.21; ESI$^+$-MS: 476.11 $[M+H]^+$ for $C_{24}H_{23}BrN_5O$.

7-((1-(4-Chlorophenyl)-1H-1,2,3-triazol-4-yl)methoxy)-1-methyl-9-propyl-9H-pyrido[3,4-b]indole (3g)

Brown powder; yield 74%; IR: ν (cm^{-1}) 1619, 1559, 1438, 1407, 1218, 1138; ^{1}H NMR (400 MHz, $CDCl_3$): δ 1.03 (t, 3H, *J* = 7.3 Hz), 1.85–1.91 (m, 2H), 3.05 (s, 3H), 4.45 (t, 2H, *J* = 7.9 Hz), 5.47 (s, 2H), 6.98–7.02 (m, 1H), 7.08 (d, 1H, *J* = 2.1 Hz), 7.51–7.54 (m, 2H), 7.72 (dd, 2H, *J* = 9.8, 3.4 Hz), 7.78 (d, 1H, *J* = 5.4 Hz), 8.02 (d, 1H, *J* = 8.5 Hz), 8.11 (s, 1H), 8.31 (s, 1H); ^{13}C NMR (100 MHz, $CDCl_3$): δ 11.25, 22.96, 23.94, 46.48, 62.43, 94.86, 109.36, 112.45, 115.62, 120.93, 121.74, 122.62, 130.01, 134.81, 135.41, 137.67, 143.23, 145.06, 159.37; ESI$^+$-MS: 432.16 $[M+H]^+$ for $C_{24}H_{23}ClN_5O$.

7-((1-Benzyl-1H-1,2,3-triazol-4-yl)methoxy)-9-butyl-1-methyl-9H-pyrido[3,4-b]indole (4a)

Brown powder; yield 85%; IR: ν (cm^{-1}) 1619, 1558, 1442, 1254, 1198; ^{1}H NMR (500 MHz, $CDCl_3$): δ 1.00 (t, 3H, *J* = 6.8 Hz), 1.44–1.48 (m, 2H), 1.80 (s, 2H), 2.94 (s, 3H), 4.48 (s, 2H), 5.33 (s, 2H), 5.56 (s, 2H), 6.93 (d, 1H, *J* = 8.1 Hz), 6.98 (s, 1H), 7.29–7.30 (m, 3H), 7.34–7.39 (m, 4H), 7.65 (s, 1H), 8.01 (d, 1H, *J* = 9.1 Hz); ^{13}C NMR (125 MHz, $CDCl_3$): δ 13.94, 20.23, 32.78, 44.69, 54.45, 62.50, 95.70, 109.57, 128.17, 128.23, 128.32, 128.84, 128.89, 129.17, 134.38, 159.32; ESI$^+$-MS: 426.23 $[M+H]^+$ for $C_{26}H_{28}N_5O$.

7-((1-(4-Bromobenzyl)-1H-1,2,3-triazol-4-yl)methoxy)-9-butyl-1-methyl-9H-pyrido[3,4-b]indole (4b)

Yellow powder; yield 83%; IR: ν (cm^{-1}) 1617, 1559, 1498, 1440, 1260, 1196; ^{1}H NMR (400 MHz, $CDCl_3$): δ 1.00 (t, 3H, *J* = 7.3 Hz), 1.41–1.49 (m, 2H), 1.76–1.84 (m, 2H), 3.04 (s, 3H), 4.46 (t, 2H, *J* = 7.7 Hz), 5.36 (s, 2H), 5.51 (s, 2H), 6.94 (dd, 1H, *J* = 8.5, 2.0 Hz), 7.00–7.01 (m, 1H), 7.15–7.17 (m, 2H), 7.49–7.53 (m, 2H), 7.62 (s, 1H), 7.80 (s, 1H), 7.99 (d, 1H, *J* = 8.5 Hz), 8.32 (s, 1H); ^{13}C NMR (100 MHz, $CDCl_3$): δ 13.92, 20.18, 32.72, 44.70, 53.57, 62.42, 94.98, 109.32, 122.35, 122.95, 129.72, 131.93, 132.26, 133.48, 143.17, 159.31; ESI$^+$-MS: 504.14 $[M+H]^+$ for $C_{26}H_{27}BrN_5O$.

9-Butyl-7-((3-(2-chlorobenzyl)-3H-1,2,4-triazol-5-yl)methoxy)-1-methyl-9H-pyrido[3,4-b]indole (4c)

Yellow powder; yield 74%; IR: ν (cm^{-1}) 1619, 1559, 1496 1442, 1254, 1442; ^{1}H NMR (500 MHz, CD_3OD): δ 0.98 (t, 3H, *J* = 7.4 Hz), 1.40–1.48 (m, 2H), 1.74–1.82 (m, 2H), 3.03 (s, 3H), 4.52–4.56 (m, 2H), 5.36 (s, 2H), 5.76 (s, 2H), 6.98–7.01 (m, 1H), 7.19 (s, 1H), 7.25 (dd, 1H, *J* = 7.6, 1.8 Hz), 7.28–7.31(m, 1H), 7.34–7.37 (m, 2H), 7.45–7.48 (m, 2H), 8.07 (d, 1H, *J* = 8.6 Hz), 8.14 (s, 1H); ^{13}C NMR (125 MHz, CD_3OD): δ 12.83, 19.63, 32.49, 44.21, 51.25, 61.51, 78.07, 94.54, 110.69, 122.47, 127.01, 127.32, 129.56, 130.08, 130.27, 144.11, 160.32; ESI$^+$-MS: 460.19 $[M+H]^+$ for $C_{26}H_{27}ClN_5O$.

9-Butyl-7-((1-(4-chlorophenyl)-1H-1,2,3-triazol-4-yl)methoxy)-1-methyl-9H-pyrido[3,4-b]indole (4d)

Greenish yellow; yield 76%; IR: ν (cm^{-1}) 1619, 1559, 1517, 1442, 1254, 1140; ^{1}H NMR (400 MHz, $CDCl_3$): δ 0.95 (t, 3H, *J* = 7.3 Hz), 1.35–1.46 (m, 2H), 1.71–1.79 (m, 2H), 2.99 (s, 3H), 4.30–4.39 (m, 2H), 5.40 (s, 2H), 6.90–6.99 (m, 2H), 7.27 (d, 1H, *J* = 8.8 Hz), 7.45 (d, 2H, *J* = 8.2 Hz), 7.66 (d, 2H, *J* = 8.3 Hz), 7.71–7.74 (m, 1H), 7.94 (d, 1H, *J* = 8.5 Hz), 8.12 (s, 1H); ^{13}C NMR (100 MHz, $CDCl_3$): δ 13.80, 20.18, 32.74, 44.72, 62.26, 94.69, 109.23, 115.51, 120.23, 121.06, 121.59, 122.50, 129.78, 129.92, 134.64, 135.31, 143.05, 144.94, 159.27; ESI$^+$-MS: 446.17 $[M+H]^+$ for $C_{25}H_{25}ClN_5O$.

7-((1-Benzyl-1H-1,2,3-triazol-4-yl)methoxy)-9-isobutyl-1-methyl-9H-pyrido[3,4-b]indole (5a)

Yellow powder; yield 81%; IR: ν (cm^{-1}) 1624, 1559, 1506, 1442, 1236; ^{1}H NMR (400 MHz, $CDCl_3$): δ 0.89 (d, 6H, *J* = 6.6 Hz), 2.19–2.25 (m, 1H), 2.98 (s, 3H), 4.23 (d, 2H, *J* = 7.5 Hz), 5.31 (s, 2H), 5.52 (s, 2H), 6.91 (dd, 1H, *J* = 8.6, 2.1 Hz), 6.99 (d, 1H, *J* = 2.1 Hz), 7.26 (dd, 2H, *J* = 6.9, 2.8 Hz), 7.33–7.37 (m, 3H), 7.59 (s, 1H), 7.72 (d, 1H, *J* = 5.2 Hz), 7.94 (d, 1H, *J* = 8.6 Hz), 8.28 (d, *J* = 5.4 Hz, 1H); ^{13}C NMR (100 MHz, $CDCl_3$): δ 20.15, 23.58, 30.56, 51.80, 54.25, 65.52, 109.24, 112.26, 115.37, 122.28, 122.78, 128.11, 128.81, 129.13, 129.29, 134.43, 138.10, 140.70, 143.41, 144.39, 159.14; ESI$^+$-MS: 426.23 $[M+H]^+$ for $C_{26}H_{28}N_5O$.

7-((1-(4-Bromobenzyl)-1H-1,2,3-triazol-4-yl)methoxy)-9-isobutyl-1-methyl-9H-pyrido[3,4-b]indole (5b)

Brown powder; yield 78%; IR: ν (cm^{-1}) 1623, 1559, 1443, 1243, 1138; ^{1}H NMR (500 MHz, $CDCl_3$): δ 0.92 (d, 6H, *J* = 6.5 Hz), 2.21–2.27 (m, 1H), 2.99 (s, 3H), 4.28 (d, 2H, *J* = 7.2 Hz), 5.35 (s, 2H), 6.93 (d, 1H, *J* = 8.5 Hz), 7.01 (s, 1H), 7.16 (d, 2H, *J* = 7.9 Hz), 7.50 (d, 2H, *J* = 7.8 Hz), 7.60 (s, 1H), 7.84 (s, 1H), 7.98 (d, 1H, *J* = 8.6 Hz); ^{13}C NMR (125 MHz, $CDCl_3$): δ 20.17, 30.58, 51.84, 53.60, 62.53, 76.80, 95.59, 109.21, 122.26, 122.71, 123.04, 129.71, 132.34, 133.42, 159.03; ESI$^+$-MS: 504.14 $[M+H]^+$ for $C_{26}H_{27}BrN_5O$.

4-((4-(((9-Isobutyl-1-methyl-9H-pyrido[3,4-b]indol-7-yl)oxy)methyl)-1H-1,2,3-triazol-1-yl)methyl)benzonitrile (5c)

Brown powder; yield 75%; IR: ν (cm^{-1}) 1621, 15559, 1443, 1408, 1192, 1138; ^{1}H NMR (400 MHz, $CDCl_3$): δ 0.88 (d, 6H, *J* = 6.5 Hz), 2.16–2.22 (m, 1H), 2.96 (s, 3H), 4.22 (d, 2H, *J* = 7.3 Hz), 5.31 (s, 2H), 5.58 (s, 2H), 6.89 (dd, 1H, *J* = 8.6, 2.1 Hz), 6.97 (d, 1H, *J* = 2.1 Hz), 7.32 (d, 2H, *J* = 7.9 Hz), 7.61 (d, 2H, *J* = 8.1 Hz), 7.68 (s, 1H), 7.76 (s, 1H), 7.93 (d, 1H, *J* = 8.5 Hz), 8.26 (s, 1H); ^{13}C NMR (100 MHz, $CDCl_3$): δ 201.5, 30.57, 51.78, 53.44, 62.38, 95.45, 109.17, 112.72, 115.48, 118.11, 128.43, 132.84, 139.66, 143.42, 159.02; ESI$^+$-MS: 451.22 $[M+H]^+$ for $C_{27}H_{27}N_6O$.

7-((1-(4-Bromophenyl)-1H-1,2,3-triazol-4-yl)methoxy)-9-isobutyl-1-methyl-9H-pyrido[3,4-b]indole (5d)

Brown powder; yield 88%; IR: ν (cm^{-1}) 1621, 1559, 1444, 1408, 1192, 1138; ^{1}H NMR (500 MHz, $CDCl_3$): δ 0.91 (d, 6H, *J* = 6.6 Hz), 2.20–2.25 (m, 1H), 2.99 (s, 3H), 4.26 (d, 2H, *J* = 7.5 Hz), 5.42 (s, 2H), 6.97 (dd, 1H, *J* = 8.6, 2.1 Hz), 7.03 (d, 1H, *J* = 2.1 Hz), 7.60–7.65 (m, 4H), 7.82 (s, 1H), 7.98 (d, 1H, *J* = 8.6 Hz), 8.09 (s, 1H), 8.37 (s, 1H); ^{13}C NMR (125 MHz, $CDCl_3$): δ 20.18, 30.60, 51.84, 62.39, 95.50, 109.17, 115.57,

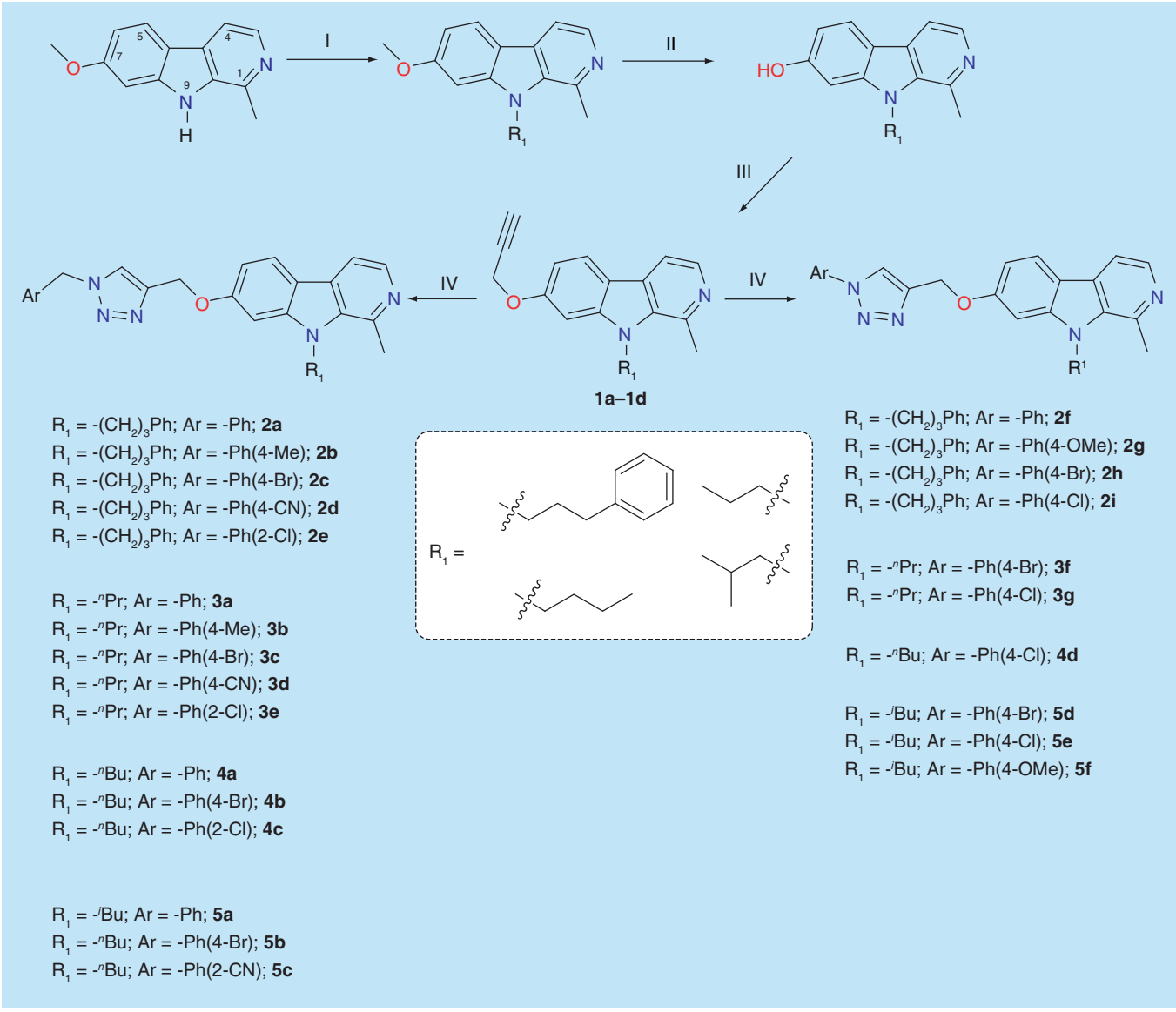

Figure 2. The synthetic route and newly synthesized harmine-based triazoles. Reagents and conditions: **(I)**. R_1-Br, NaH, DMF, reflux; **(II)**. HBr, AcOH, 115°C, 15h; **(III)**. Cs_2CO_3, DMF, propargyl bromide, 60°C, 3h; **(IV)**. $ArCH_2N_3$ or ArN_3, $CuSO_4.5H_2O$, sodium ascorbate, THF-H_2O (1:1), rt.

120.87, 121.89, 122.38, 122.59, 129.16, 132.93, 135.83, 143.44, 145.12, 158.99; ESI$^+$-MS: 490.12 $[M+H]^+$ for $C_{25}H_{25}BrN_5O$.

7-((1-(4-Chlorophenyl)-H-1,2,3-triazol-4-yl)methoxy)-9-isobutyl-1-methyl-9H-pyrido[3,4-b]indole (5e)

Yellow powder; yield 78%; IR: ν (cm^{-1}) 1619, 1559, 1442, 1407, 1196, 1140; ^{1}H NMR (500 MHz, $CDCl_3$): δ 0.90 (d, 6H, J = 6.7 Hz), 2.20–2.24 (m, 1H), 2.98 (s, 3H), 4.24 (d, 2H, J = 7.5 Hz), 5.41 (s, 2H), 6.95 (dd, 1H, J = 8.6, 2.2 Hz), 7.02 (d, 1H, J = 2.2 Hz), 7.45–7.48 (m, 2H), 7.65–7.68 (m, 2H), 7.72 (d, 1H, J = 5.2 Hz), 7.96 (d, 1H, J = 8.5 Hz), 8.08 (s, 1H), 8.29 (d, 1H, J = 5.3 Hz); ^{13}C NMR (125 MHz, $CDCl_3$): δ 20.17, 23.61, 30.59, 51.82, 62.37, 76.87, 95.45, 109.13, 112.27, 115.52, 120.95, 121.64, 122.37, 129.23, 129.94, 134.67, 135.34, 135.63, 138.22, 140.79, 143.38, 145.05, 158.98; ESI$^+$-MS: 446.17 $[M+H]^+$ for $C_{25}H_{25}ClN_5O$.

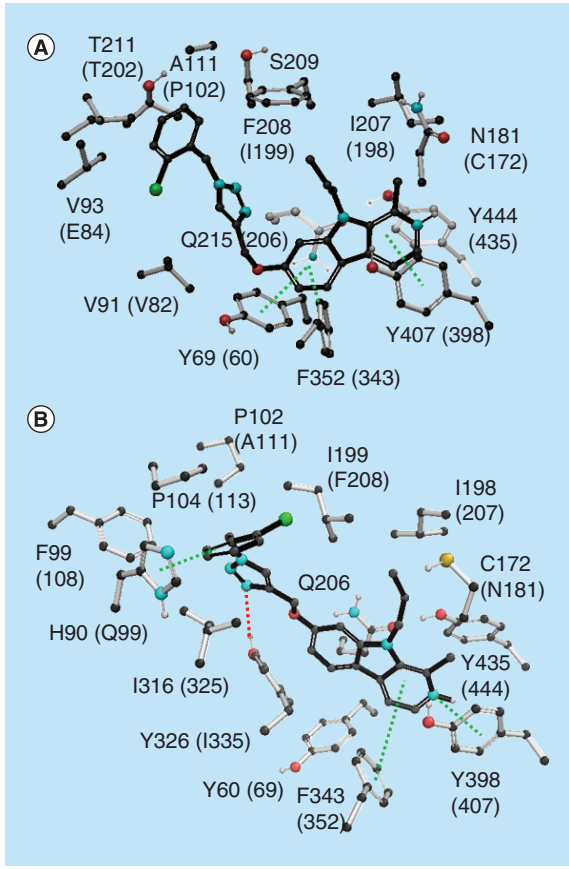

Figure 3. Key interactions of compound 3e in MAO-A (A) and MAO-B (B) isoforms.

9-Isobutyl-7-((1-(4-methoxyphenyl)-1H-1,2,3-triazol-4-yl)methoxy)-1-methyl-9H-pyrido[3,4-b]indole (5f)

White powder; yield 80%; IR: ν (cm^{-1}) 1624, 1558, 1504, 1442, 1243; ^{1}H NMR (400 MHz, $CDCl_3$): δ 0.89 (d, 6H, *J* = 6.6 Hz), 2.17–2.24 (m, 1H), 2.98 (s, 3H), 3.82 (s, 3H), 4.23 (d, 2H, *J* = 7.4 Hz), 5.39 (s, 2H), 6.94–6.99 (m, 3H), 7.03 (d, 1H, *J* = 2.1 Hz), 7.57–7.61 (m, 2H), 7.74 (s, 1H), 7.96 (d, 1H, *J* = 8.6 Hz), 8.01 (s, 1H), 8.30(s, 1H); ^{13}C NMR (100 MHz, $CDCl_3$): δ 20.15, 30.58, 51.80, 55.60, 62.45, 95.48, 109.30, 114.76, 115.39, 121.25, 122.14, 122.23, 122.34, 129.32, 130.31, 143.47, 144.48, 159.15, 159.89; ESI$^+$-MS: 442.22 $[M+H]^+$ for $C_{26}H_{28}N_5O_2$.

MAO assay

To examine the inhibitory effect of harmine analogs on MAO-A and -B, the kynuramine deamination assay was adapted for 384-well plates as described earlier [18–20]. Human MAO-A and -B enzymes were purchased from BD Biosciences (MA, USA). The controls, Kynuramine, clorgyline, deprenyl, phenelzine and DMSO were procured from Sigma Chemical (MO, USA). Appropriate controls with the test compounds were included to check the possible interference with the fluorescence measurements. None of the test compounds showed any interference with fluorescence measurement. The determination of IC_{50} values for inhibition of MAO-A and -B by the harmine analogs was determined using fixed concentration of the substrate, kynuramine (80/50 μM) and varying concentrations (0.01–100 μM) of the inhibitor/test compounds. Harmine analogs (0.001–100 μM), clorgyline (0.001–100 μM) and harmine (0.0001–100 μM) for MAO-A and harmine analogs (0.0001–100 μM), deprenyl (0.001–100 μM) and harmine (0.1–100 μM) for MAO-B were tested to determine the IC_{50}, from the dose–response inhibition curves using XL-Fit© software.

In silico docking

The 3D crystal structures of MAO-A (2Z5X) at a resolution of 2.2 Å and MAO-B (2V61) at a resolution of 1.7Å, were downloaded from the protein data bank [8,15]. The crude structures were prepared using Protein Preparation Wizard in the Schrodinger suite 2015–3. In order to prepare the proteins, the hydrogen atoms were added after

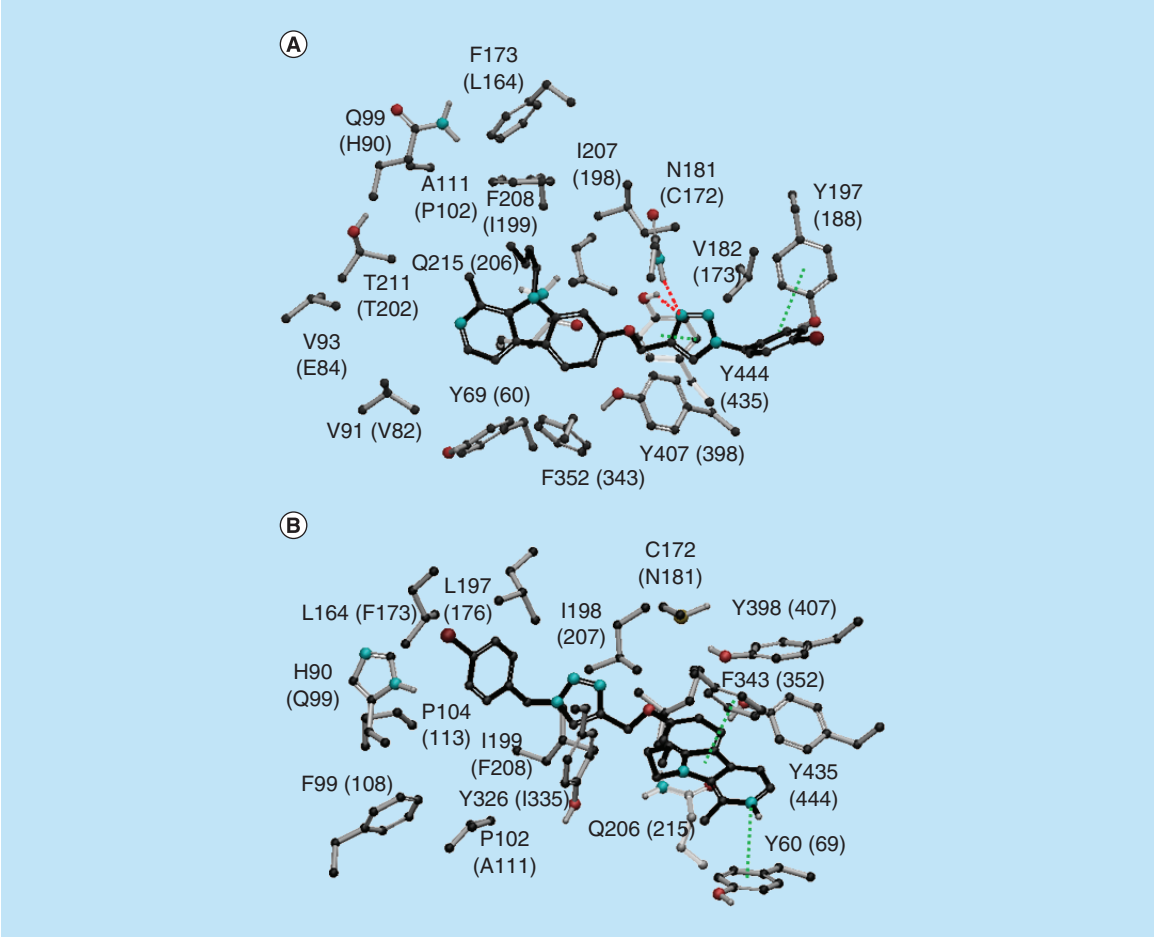

Figure 4. Key interactions of compound 4b in MAO-A (A) and MAO-B (B) isoforms.

deleting the original ones. The protein was checked and some missing side chains and loop segments were added using prime. This was followed by the adjustment of the bond orders for amino acid residues and the ligand. The protonated and tautomeric states were adjusted to match a pH 7.4. Moreover, the protein–ligand complex was subjected to geometry refinement using an Optimized Potential for Liquid Simulations (OPLS 2005) force field followed by the restrained minimization for the hydrogens only. The 2D structures of the 26 analogs were sketched using ChemDraw Professional 15.0 and then converted to 3D structures using Chem 3D 15.0. They were then imported to Maestro. The analysis of different conformers, tautomers and ionization states of each molecule was carried out using LigPrep. After the protein and ligand preparation Induced Fit Docking protocol was operated to obtain the best docking solution for each molecule. The grid box was auto sized and centered on the crystallized ligand. Ligand conformational sampling was carried out in a range of 2.5 Kcal/mol. Both receptor and ligands were softened by a scaling factor of 5 Å. A maximum of five poses was saved for each molecule. The surrounding residues spotted in a distance of 6 Å from the ligand were refined using prime to allow for flexibility. Glide standard precision (SP) mode was used for the redocking step into the top five receptor structures generated within 30 Kcal/mol of the best structure by the prime refinement. Validation of the (Induced Fit Docking) protocol was accommodated by a redocking step, where the native ligands in both crystal structures were redocked to generate root mean square distance values of 0.268 Å for MAO-A and 1.438 Å for MAO-B isoforms.

Results & discussion

Chemistry

A focused library of 26 novel harmine-conjugated 1,2,3-triazoles has been synthesized starting from harmine. As shown in Figure 2, harmine was *N*-alkylated with selective alkyl halides, namely, 1-bromo-3-phenylpropane,

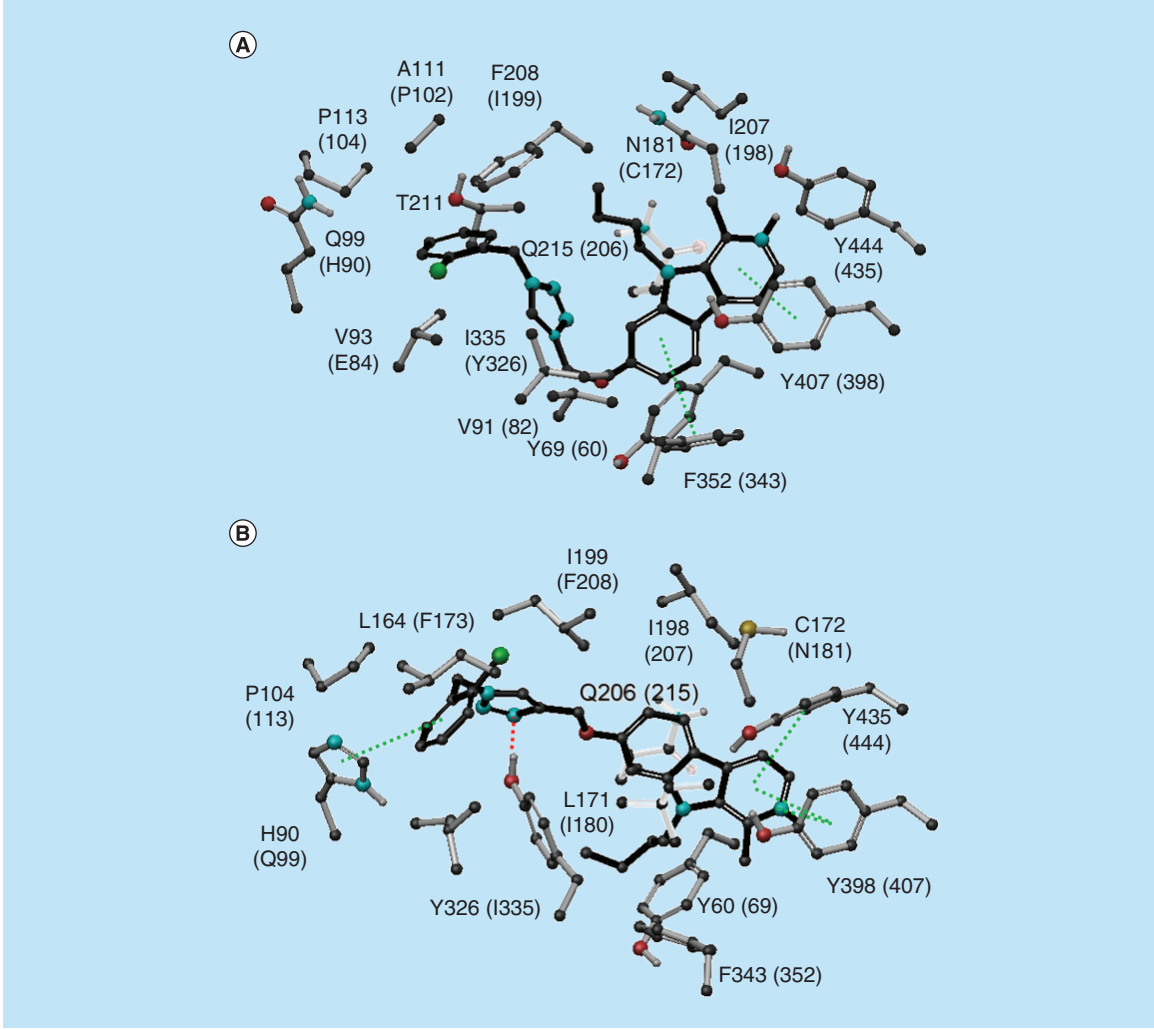

Figure 5. Key interactions of compound 4c in MAO-A (A) and MAO-B (B) isoforms.

1-bromopropane, 1-bromobutane and 1-bromo-2-methylpropane using sodium hydride as a base (Figure 2, Step I). These alkyl halides were selected on the basis of earlier reports of MOA, DYRK1A and anticancer activities of harmine analogs [21–25]. In 2017, Kotschy and his team outlined the modifications to harmine scaffold with different selectivity, inhibitory profiles for kinase and monoamine oxidases [21–25]. The alkylated harmine was then subjected to selective *O*-demethylation by refluxing with HBr in AcOH (Figure 2, Step II) followed by *O*-propargylation with Cs_2CO_3 as a base (Figure 2, Step III). The presence of two doublets at δ 4.76–4.85 for the OCH_2 and broad triplet between δ 2.57 and 2.60 for the terminal C$\underline{H}$ group in the ^{1}H NMR and presence of carbon signals in a region of δ 75–78 (C≡C) and δ 56.23–56.33 ($O\underline{C}H_2$) confirmed the formation of a key propargyl intermediate. These propargylated intermediates were then functionalized with several readily available azides to yield the target compounds via 'click' chemistry (Figure 2, Step IV). The formation of the final harmine-based 1,2,3-triazole derivatives was confirmed by the absence of the triplet signal (1H) for terminal alkyne and the presence of singlet (1H) for the triazolyl proton in the region of δ 7.56–7.78 in the ^{1}H NMR. The structural assignment was also supported by the ^{13}C NMR spectral data, which showed the C-atom signals corresponding to carbon atoms in 1,2,3-triazole derivatives and the final confirmation was made by the ESI–MS analysis (Supplementary Figures 2 & 3). As expected, only the sterically stable, regio-isomer, 1,4-disubstituted 1,2,3-triazole(s) was isolated and its structure(s) was confirmed with nuclear Overhauser effect spectroscopy (NOSEY) experiments wherein no correlations between OCH_2 protons with *N*-aryl protons were observed (Supplementary Figure 4).

Table 1. Inhibition of recombinant human MAO-A and -B by harmine-conjugated 1,2,3-triazoles.

Compounds	MAO-A IC_{50}(μM)	MAO-B IC_{50}(μM)	Selectivity index MAO-A/MAO-B
2a	>100	30.76 ± 3.27	–
2b	69.45 ± 2.53	8.21 ± 2.31	8.46
2c	3.83 ± 0.04	43.65 ± 2.36	0.09
2d	>100	>100	–
2e	60.91 ± 0.62	38.29 ± 3.19	1.59
2f	60.50 ± 3.09	39.65 ± 9.59	1.53
2g	39.50 ± 1.50	21.32 ± 2.76	1.85
2h	4.19 ± 0.16	58.08 ± 1.55	0.07
2i	>100	58.11 ± 11.45	–
3a	3.61 ± 0.03	9.55 ± 1.19	0.38
3b	**1.53 ± 0.17**	**1.21 ± 0.14**	1.26
3c	7.78 ± 0.25	11.87 ± 3.50	0.66
3d	>100	>100	–
3e	**0.83 ± 0.03**	**0.26 ± 0.04**	3.20
3f	3.94 ± 0.32	9.17 ± 0.04	0.43
3g	1.69 ± 0.02	7.93 ± 0.38	0.21
4a	1.30 ± 0.05	1.89 ± 0.02	0.69
4b	1.40 ± .012	28.33 ± 0.58	0.05
4c	**0.43 ± 0.002**	**0.36 ± 0.001**	1.20
4d	1.32 ± 0.20	9.38 ± 0.48	0.14
5a	1.46 ± 0.01	1.77 ± 0.26	0.82
5b	2.68 ± 0.22	6.03 ± 0.89	0.44
5c	9.26 ± 0.06	4.04 ± 0.52	2.29
5d	0.51 ± 0.05	2.96 ± 0.23	0.17
5e	0.86 ± 0.03	2.26 ± 0.72	0.38
5f	**0.56 ± 0.02**	**1.08 ± 0.02**	0.52
Harmine	**0.0043 ± 0.0003**	**22.33 ± 3.21**	0.00019
Clorgyline	0.0048 ± 0.0006	–	–
Deprenyl	–	0.0530 ± 0.008	–

IC_{50} values are expressed as mean with mean ± SD of triplicate observations. Compounds with significant biological activity are highlighted as bold font.

MAO inhibition

The newly synthesized harmine-conjugated 1,2,3-triazole derivatives were subjected to *in vitro* screening for their inhibitory effect against recombinant human MAO isoforms (MAO-A and -B). The enzymatic activity of MAO-A and -B was determined by a kynuramine-based fluorescent assay method [26]. To assess the 50% inhibition of MAO isoform enzymatic activity, the IC_{50} values for the newly synthesized harmine analogs were measured and are outlined in Table 1. In general, the inhibitory effects of all newly synthesized harmine-conjugated 1,2,3-triazole derivatives against MAO-B were found to be more potent than the parent harmine, which exhibited an IC_{50} of 22.33 ± 3.21 μM. These substitutions resulted into marked loss of activity (ranging from 100- to 1000-fold) against MAO-A but significantly improved the activity against MAO-B (up to 85-fold, compound **3e**). The compounds **2h** and **4b** exhibited a higher selectivity against MAO-A with a selectivity index (**MAO-A/B**) of 0.07 and 0.05 respectively in comparison to the other compounds. The compounds **3b** (18%), **3e** (84%), **4c** (61%) and **5f** (20%) were found to exhibit more potent inhibition of MAO-B as compared with the parent alkaloid, harmine.

Compounds **2a –2i,** containing a bulky 3-phenylpropyl group at the ninth position of the harmine nucleus, did not exhibit MAO inhibition in comparison to those containing smaller *n*-butyl, *n*-propyl or *iso*-butyl groups at the same position. Compounds **2d**, **3d** and **5c** containing the electron-withdrawing cyano group on the para position of the aromatic ring attached with the triazolyl ring exhibited the least MAO inhibition. These observations are in agreement with reported results on rasagiline with selectivity index of 0.07 by Binda *et al.* [27]. Rasagiline is an irreversible, MAO-B selective inhibitor that has been approved as a novel anti-Parkinson's drug. Interestingly, the MAO inhibitory activity was found to decrease in the order **3b**>**3a**>**3c**, indicating that an electron-donating group

such as the methyl group on the aromatic ring is preferred at this position over unsubstituted aromatic ring (**3a**) followed by the least potent weakly electron withdrawing bromo atom (**3c**). Another interesting structure–activity relationship (SAR) observation is that the conjugates with one methylene group between harmine, triazole nucleus is preferred (**2f** and **3f**) over those with double methylene bridge **2a** and **3c**.

Docking studies & molecular insights

In order to assess the putative binding mode of the newly synthesized molecules with MAO proteins, the compounds have been docked against both isoforms of MAO (MAO-A [PDB: 2Z5X] and MAO-B [PDB: 2V61]] crystal structures. Even though, harmine is reported to be a reversible MAO-A inhibitor, the co-crystallized structure (2Z5X) does not exhibit any ionic interactions. However, harmine possess network of hydrophobic interactions with residues Tyr407, Phe208, Phe352, Tyr69, Tyr44, Ile180, Ile335, Leu337, Ile325 and Val210. Due to these interactions, harmine is firmly situated inside the substrate cavity near the FAD cofactor. Two water molecules are involved in stabilization of harmine–FAD interactions via hydrogen bonding. Further, the π–π interactions between the aromatic rings and the amide group of Glu215 with interplaner distance of 3.4 Å strengthens the noncovalent interactions of harmine inside the pocket.

Safinamide and coumarin analogs appended with benzyloxy group were reported to be selective MAO-B inhibitors (Figure 1) (PDB: 2V61). The isoform selectivity was attributed to the fact that these small molecules occupy both cavities unique to the bipartite binding site found in MAO-B, but not in MAO-A. The first cavity is filled with the coumarin part of the ligand with the pyran ring oxygen pointing toward Tyr326 at the top of the cavity and aligned with Tyr60 and Gln206. The secondary amine substituent at position 4 is sandwiched by the aromatic pair Tyr398-Tyr435 and interaction with Cys172. Regarding the second cavity, the benzyloxy group attached to the coumarin occupies the entrance cavity and interacts with Leu171, Ile199 and Ile316. Compound **3e** was found to exhibit π–π interactions (Figure 3) with Phe352, Tyr69 and Tyr407 amino acid residues which in turn reflects its *in vitro* IC_{50} of 0.83 μM in MAO-A. Whereas, compound **3e** was found to exhibit π–π interactions with His90 and Phe343 along with hydrogen bonding with Tyr326 in MAO-B (Figure 3) with an IC_{50} of 0.26 μM. Compound **4b** was found to exhibit hydrogen bonding (Figure 4) with Asn181 and Tyr444 along with π–π interaction with Tyr197 and Tyr444 in MAO-A crystal structure. The results of the *in vitro* MAO-A activity revealed that compound **4b** is selective toward MAO-A over MAO-B (IC_{50} 1.40 μM in MAO-A vs 28.33 μM against MAO-B). In MAO-B crystal structure, **4b** exhibits only one ion–π interaction with Tyr60 and no hydrogen bonding. Compound **4c** exhibited π–π interaction with Phe352 and Tyr407 against MAO-A isoform, whereas, hydrogen bonding interactions with Tyr326 and π–π stacking with His90, Tyr398 and Tyr435 in MAO-B isoform were noticed (Figure 5).

Conclusion

In summary, a focused library of 26 harmine scaffold tethered with triazole functionality were synthesized in order to assess their MAO inhibition. Several newly synthesized analogs showed preference toward both isoforms of MAO with micromolar to sub-micromolar inhibition. However, the potency and specificity to MAO-A was lost in these newly synthesized C7-modified harmine analogs. The MAO-inhibition data were further explained with the help of *in silico* studies using MAO-A and -B crystal structure and docking studies. The synthesized compounds were found to exhibit π–π interactions and hydrogen bonding with amino acid residues like Asn181, His90, Phe343, His90, Tyr398 and Tyr435 –among others, in the binding pocket. It appears that the modification at C-9 is not necessary and NH is essential for retaining the selectivity toward MAO-A inhibition.

Future perspective

β-Carboline harmala alkaloids and their synthetic analogs are found to be important chemical probes for the identification of biological targets, such as MAO-A, topoisomerase I, cyclin-dependent kinases, 5-hydroxytryptamine uptake, benzodiazepine and imidazoline receptors. Recently, harmine was identified as a potent inhibitor of DYRK1A with remarkable selectivity over other kinases and inhibition of such biological targets has been implicated to therapeutic options for the treatment of Down syndrome and other neurological disorders. Conversely, evidences indicate that harmala alkaloids are implicated in diverse toxicological effects as well as behavioral changes in vertebrates, that includes cytotoxicity and neurotoxicity. The chemistry and results presented here along with literature reports suggest that it is possible to design and synthesize harmine analogs with different selectivity profiles. For example, to abolish the MAO-A selectivity, block the formation of O-sulfate harmine metabolite, a

major metabolite across all species, introduction of bulky, nonmetabolic functional groups would be ideal. Such a strategy might be helpful in designing harmine-based therapeutic drugs without adverse effects.

Summary points

- **Rationale:** keeping in mind the selective inhibitory activity of harmine on MAO-A, we have designed the synthesis of single and double methylene-bridged 1,2,3-triazole derivatives through 'click' chemistry, and screened them for their MAO inhibitory potentials.
- **Results:** the inhibitory effects of all newly synthesized harmine-conjugated 1,2,3-triazole derivatives against MAO-B were found to be more potent than the parent harmine. Compounds **2h** and **4b** exhibited a higher selectivity against MAO-A with a selectivity index (MAO-A/B) of 0.07 and 0.05 respectively in comparison to the other compounds.
- **Molecular docking:** the synthesized compounds were found to exhibit π–π interactions and hydrogen bonding with amino acid residues like Asn181, His90, Phe343, His90, Tyr398 and Tyr435 – among others, in the binding pocket.

Acknowledgements

The authors would like to thank Professor J Parcher for the editing, proof-reading and valuable suggestions for improving the quality of the manuscript.

Financial & competing interests disclosure

This study was supported in part by 1R01CA173499-01A1, NIH and United States Department of Agriculture (USDA), Agricultural Research Service, Specific Cooperative Agreement 58-6060-6-015. This study was also supported in part by grant number P20GM104932 from the National Institute of General Medical Sciences (NIGMS), a component of the NIH. The content is solely the responsibility of the authors and does not necessarily represent the official views of the NIH, USDA or National Institute of General Medical Sciences. The authors have no other relevant affiliations or financial involvement with any organization or entity with a financial interest in or financial conflict with the subject matter or materials discussed in the manuscript apart from those disclosed.

No writing assistance was utilized in the production of this manuscript.

References

Papers of special note have been highlighted as: • of interest; •• of considerable interest

1. Asgarpanah J, Ramezanloo F. Chemistry, pharmacology and medicinal properties of Peganum harmala L. *Afr. J. Pharm. Pharmacol.* 6(22), 1573–1580 (2012).
2. Bongiorno De Pfirter GM, Mandrile EL. Natural active principles with hallucinogenic action: V. Harmine and harmaline. Their presence in Banisteriopsis genus species (Malpighiaceae). *Acta Farm. Bonaerense* 3(2), 161–168 (1984).
3. Airaksinen MM, Kari I. β-carbolines, psychoactive compounds in the mammalian body. Part I: occurrence, origin and metabolism. *Med. Biol.* 59(1), 21–34 (1981).
4. Moloudizargari M, Mikaili P, Aghajanshakeri S, Asghari MH, Shayegh J. Pharmacological and therapeutic effects of *Peganum harmala* and its main alkaloids. *Pharmacogn. Rev.* 7(14), 199–212 (2013).

• **Excellent review article on harmala alkaloids and their therapeutic effects.**

5. Bain J, Plater L, Elliott M *et al.* The selectivity of protein kinase inhibitors: a further update. *Biochem. J.* 408(3), 297–315 (2007).
6. Miralles A, Esteban S, Sastre-Coll A, Moranta D, Asensio VJ, Garcia-Sevilla JA. High-affinity binding of β-carbolines to imidazoline I2B receptors and MAO-A in rat tissues: norharman blocks the effect of morphine withdrawal on DOPA/noradrenaline synthesis in the brain. *Eur. J. Pharmacol.* 518(2–3), 234–242 (2005).
7. Ogawa Y, Nonaka Y, Goto T *et al.* Development of a novel selective inhibitor of the Down syndrome-related kinase Dyrk1A. *Nat. Commun.* 1, 86 (2010).
8. Son SY, Ma J, Kondou Y, Yoshimura M, Yamashita E, Tsukihara T. Structure of human monoamine oxidase A at 2.2-A resolution: the control of opening the entry for substrates/inhibitors. *Proc. Natl Acad. Sci. USA* 105(15), 5739–5744 (2008).
9. Westlund KN, Denney RM, Kochersperger LM, Rose RM, Abell CW. Distinct monoamine oxidase A and B populations in primate brain. *Science* 230(4722), 181–183 (1985).
10. Bach AW, Lan NC, Johnson DL *et al.* cDNA cloning of human liver monoamine oxidase A and B: molecular basis of differences in enzymatic properties. *Proc. Natl Acad. Sci. USA* 85(13), 4934–4938 (1988).

11. Greenawalt JW, Schnaitman C. An appraisal of the use of monoamine oxidase as an enzyme marker for the outer membrane of rat liver mitochondria. *J. Cell Biol.* 46(1), 173–179 (1970).
12. Grimsby J, Chen K, Wang LJ, Lan NC, Shih JC. Human monoamine oxidase A and B genes exhibit identical exon-intron organization. *Proc. Natl Acad. Sci. USA* 88(9), 3637–3641 (1991).
13 . Kalgutkar AS, Dalvie DK, Castagnoli N Jr, Taylor TJ. Interactions of nitrogen-containing xenobiotics with monoamine oxidase (MAO) isozymes A and B: SAR studies on MAO substrates and inhibitors. *Chem. Res. Toxicol.* 14(9), 1139–1162 (2001).
14. Reniers J, Robert S, Frederick R, Masereel B, Vincent S, Wouters J. Synthesis and evaluation of β-carboline derivatives as potential monoamine oxidase inhibitors. *Bioorg. Med. Chem.* 19(1), 134–144 (2011).
15. Binda C, Wang J, Pisani L *et al.* Structures of human monoamine oxidase B complexes with selective noncovalent inhibitors: safinamide and coumarin analogs. *J. Med. Chem.* 50(23), 5848–5852 (2007).

•• **Informative research article on selective monoamine oxidase-B noncovalent inhibitors.**

16. Agalave SG, Maujan SR, Pore VS. Click chemistry: 1,2,3-triazoles as pharmacophores. *Chem. Asian J.* 6(10), 2696–2718 (2011).

•• **Good review article on importance of 1,23-triazoles as pharmacophores.**

17. Dheer D, Singh V, Shankar R. Medicinal attributes of 1,2,3-triazoles: current developments. *Bioorg. Chem.* 71 30–54 (2017).
18. Chaurasiya ND, Gogineni V, Elokely KM *et al.* Isolation of acacetin from *Calea urticifolia* with inhibitory properties against human monoamine oxidase-A and -B. *J. Nat. Prod.* 79(10), 2538–2544 (2016).
19. Chaurasiya ND, Ibrahim MA, Muhammad I, Walker LA, Tekwani BL. Monoamine oxidase inhibitory constituents of propolis: kinetics and mechanism of inhibition of recombinant human MAO-A and MAO-B. *Molecules* 19(11), 18936–18952 (2014).
20. Samoylenko V, Rahman MM, Tekwani BL *et al. Banisteriopsis caapi*, a unique combination of MAO inhibitory and antioxidative constituents for the activities relevant to neurodegenerative disorders and Parkinson's disease. *J. Ethnopharmacol.* 127(2), 357–367 (2010).
21. Balint B, Weber C, Cruzalegui F, Burbridge M, Kotschy A. Structure-based design and synthesis of harmine derivatives with different selectivity profiles in kinase versus monoamine oxidase inhibition. *ChemMedChem* 12(12), 932–939 (2017).

•• **Excellent paper on the crystal structure of MAO inhibitors.**

22. Cao R, Fan W, Guo L *et al.* Synthesis and structure–activity relationships of harmine derivatives as potential antitumor agents. *Eur. J. Med. Chem.* 60 135–143 (2013).
23. Frederick R, Bruyere C, Vancraeynest C *et al.* Novel trisubstituted harmine derivatives with original *in vitro* anticancer activity. *J. Med. Chem.* 55(14), 6489–6501 (2012).
24. Cao R, Chen Q, Hou X *et al.* Synthesis, acute toxicities, and antitumor effects of novel 9-substituted β-carboline derivatives. *Bioorg. Med. Chem.* 12(17), 4613–4623 (2004).
25. Drung B, Scholz C, Barbosa VA, Nazari A, Sarragiotto MH, Schmidt B. Computational & experimental evaluation of the structure/activity relationship of β-carbolines as DYRK1A inhibitors. *Bioorg. Med. Chem. Lett.* 24(20), 4854–4860 (2014).
26. Parikh S, Hanscom S, Gagne P, Crespi C, Patten C. A fluorescent-based, high-throughput assay for detecting inhibitors of human monoamine oxidase A and B. *BD Bioscience Discovery Labware* S02T081R082 (2002).
27. Binda C, Hubalek F, Li M *et al.* Binding of rasagiline-related inhibitors to human monoamine oxidases: a kinetic and crystallographic analysis. *J. Med. Chem.* 48(26), 8148–8154 (2005).

• **Important article on crystal structures and kinetics of rasagiline-based inhibitors for hMAO.**